HHS Public Access

Author manuscript

Heart Rhythm. Author manuscript; available in PMC 2022 January 01.

Published in final edited form as:

Heart Rhythm. 2021 January ; 18(1): 88–97. doi:10.1016/j.hrthm.2020.07.020.

Sex-specific I_{KAS} activation in rabbit ventricles with drug-induced QT prolongation

Adonis Z. Wu, PhD[1], **Mu Chen, MD**[1], **Dechun Yin, MD**[1], **Thomas H. Everett IV, PhD, FHRS**[1], **Zhenhui Chen, PhD**[1], **Michael Rubart, MD**[2], **James N. Weiss, MD**[3], **Zhilin Qu, PhD**[3], **Peng-Sheng Chen, MD, FHRS**[1,4]

[1]Krannert Institute of Cardiology and Division of Cardiology, Department of Medicine, Indiana University School of Medicine, Indianapolis, Indiana

[2]Department of Pediatrics, Riley Heart Research Center, Indiana University School of Medicine, Indianapolis, Indiana

[3]Departments of Medicine (Cardiology) and Physiology, David Geffen School of Medicine at the University of California

[4]Cedars-Sinai Medical Center, Los Angeles, CA

Abstract

Background—Female sex is a known risk factor for drug-induced long QT syndrome (diLQTS). We recently demonstrated a sex difference in apamin-sensitive small-conductance Ca^{2+}-activated K^+ (SK) current (I_{KAS}) activation during β-adrenergic stimulation.

Objective—To test the hypothesis that there is a sex difference of I_{KAS} in the rabbit models of diLQTS.

Methods—We evaluated the sex differences in ventricular repolarization from 15 male and 22 female Langendorff-perfused rabbit hearts with optical mapping techniques during atrial pacing. HMR1556 (I_{Ks} blocker), E4031 (I_{Kr} blocker) and sea anemone toxin (ATX-II, I_{NaL} activator) were used to simulate types 1-3 LQTS, respectively. Apamin, an I_{KAS} blocker was then added to determine the magnitude of further QT prolongation.

Results—HMR1556, E4031 and ATX-II led to APD_{80} prolongation in both male and female ventricles at pacing cycle lengths (PCLs) of 300-400 ms. Apamin further lengthened APD_{80} (in PCL350 ms) from 187.8±4.3 to 206.9±7.1 (p=0.014) in HMR1556 treated, from 209.9±7.8 to 224.9±7.8 (p=0.003) in E4031 treated, and from 174.3±3.3 to 188.1±3.0 (p=0.0002) in ATX-II treated female hearts. In contrast, apamin did not further lengthen the APD_{80} in male hearts. Compared with the baseline, the Ca_i transient duration (Ca_iTD) was significantly increased in diLQTS but without sex differences. There were no significant effects of apamin on Ca_iTD.

Address for Correspondence: Peng-Sheng Chen, MD, Cedars-Sinai Medical Center, Los Angeles, CA 90048, chenp@cshs.org.

Conflict of Interest: None

Conclusion—We conclude that I_{KAS} is abundantly increased in female but not in male ventricles with diLQTS. Increased I_{KAS} helps preserve the repolarization reserve in female ventricles treated with I_{Ks} and I_{Kr} blockers or I_{NaL} activators.

Keywords

Calcium transient; ion currents; optical mapping; repolarization reserve; SK current

Introduction

Drug-induced long QT syndrome (diLQTS) is the most common reason that prevents a drug from reaching the market.[1] The most common type of diLQTS is due to the inhibition of the rapid component of the delayed rectifier potassium current (I_{Kr}).[2] Cardiac repolarization is controlled by the balance between outward and inward ionic conductances during the plateau phase of the action potential.[3] Mutations of KCNQ1 (I_{Ks}), KCNH2 (I_{Kr}) and SCN5A (I_{NaL}) genes cause long QT syndrome (LQTS) types 1-3, respectively.[4] However, family members with the same genetic mutations may have vastly different QT intervals,[5, 6] indicating that other factors may potentially play a role in determining the QT interval in patients with congenital LQTS.[6-8] Apamin-sensitive small-conductance Ca^{2+}-activated K^+ channel (SK) current (I_{KAS}) is present but not active or only minimally active in the normal ventricles.[9, 10] However, I_{KAS} is abundantly present in heart failure, myocardial infarction and hypokalemia when repolarization reserve is reduced.[11-13] We recently documented that β-adrenergic stimulation activates ventricular I_{KAS} in females to a much greater extent than in males.[14] We hypothesize that (1) I_{KAS} is activated in rabbit ventricles in diLQTS, and (2) the magnitude of I_{KAS} activation during diLQTS is greater in female than in male ventricles. We performed an optical mapping study in Langendorff-perfused normal rabbit ventricles to test these hypotheses.

Methods

The study protocol was approved by the Institutional Animal Care and Use Committee of Indiana University School of Medicine and the Methodist Research Institute and conform to the Guide for the Care and Use of Laboratory Animals.

Surgical preparations

Adult New Zealand White rabbits (N=37, 2.7-3.5 Kg) were euthanized by intravenous sodium pentobarbital overdose (160 mg/kg, i.v.). Hearts were harvested and Langendorff perfused with 37°C Tyrode solution (in mmol/L: NaCl 128.3, KCl 4.7, $NaHCO_3$ 20.2, NaH_2PO_4 0.4, $CaCl_2$ 1.8, $MgSO_4$ 1.2, glucose 11.1 and bovine serum albumin 40 mg/L) bubbled with 95% O_2/5% CO_2 to maintain a pH of 7.4. All chemicals were purchased from Sigma-Aldrich (St. Louis, MO). Pseudo-electrocardiogram (pECG) was simultaneously recorded by placing widely spaced electrodes close to the right atrium (RA) and the apex of the left ventricle (LV), respectively, to determine the QT interval and ventricular rhythm. The signals were band-pass filtered between 0.5 Hz to 150 Hz with a sampling rate of 1000 Hz. The pECG traces and methods of QT measurements are shown in Figure 1.

Optical mapping

Simultaneous optical mapping of intracellular calcium (Ca_i) and membrane potential (V_m) was performed using previously reported techniques.[14] The hearts were stained with Rhod-2 AM (1.4 μmol/L, from Invitrogen, Grand Island, NY) for Ca_i mapping and RH237 (10 μmol/L, from Invitrogen, Grand Island, NY) for V_m mapping. Blebbistatin (15~20 μmol/L, from Tocris Bioscience, Minneapolis, MN) was used to inhibit contraction. The epicardial surfaces of the right and left ventricles were excited with a laser (Verdi G5, Coherent Inc., Santa Clara, CA) at a wavelength 532 nm, and the emitted fluorescence was filtered with a 715 nm long pass filter. The fluorescence was recorded with 100 x 100 pixels for a spatial resolution of 0.35 x 0.35 mm^2 per pixel at a 2-ms/frame sampling rate. Optical signals were processed with both spatial and temporal filtering. A dynamic atrial pacing protocol was performed and the optical signals were recorded at different pacing cycle lengths (PCLs).[15] When comparing action potential duration (APD) among baseline and after each treatment, we paced the right atrial at fixed PCL (S1S1) to avoid rate-dependent APD changes. The slowest pacing rate is limited by the competing sinus or escape rates of the Langendorff perfused hearts. We were unable to consistently pace with PCL longer than the sinus cycle length (250-400 ms). We started to acquire optical mapping signals after at least 30 paced beats at the same PCL. The PCLs were progressively shortened (400, 350, 300, 250, 200, and 170 ms) until the loss of 1:1 capture. APD at 80% repolarization (APD_{80}) were used for data analyses. We did not use programmed stimulation to induce arrhythmias. In all protocols, the drugs were sequentially added and recirculated in the perfusate.

Protocol-I (diLQT1): Epicardial optical signals were mapped sequentially at baseline, after adding HMR1556 (I_{Ks} blocker) to simulate type 1 LQTS, after adding apamin in the continued presence of HRM1556 and after washout. This study was performed in a total 5 male and 8 female rabbit hearts. The optical voltage signals were obtained from the anterior surface of the heart including both right ventricle (RV) and left ventricle (LV). The annotated RV/LV locations and image data acquisition procedures are shown in Online Supplement Figure 1. After baseline recording, HMR1556 (100 nmol/L) was added to the perfusate. APD measurement was performed 15 min after HMR1556 infusion. Apamin (100 nmol/L) was subsequently added in the continued presence of HMR1556. All drugs were washed out 15 min after apamin infusion. The APDs were measured at least twice in pharmacological steady-state. All experiments were completed within 1.5 hr to minimize phototoxicity induced by long-term laser exposure in these *ex vivo* ventricles.

Protocol-II (diLQT2): Epicardial mapping of both the RV and the LV was conducted at baseline, after adding E4031 (I_{Kr} blocker, 50 nmol/L), after adding apamin (100 nmol/L) in the continued presence of E4031 and after washout. This protocol was performed in 6 male and 7 female hearts.

Protocol-III (diLQT3): Epicardial mapping of both the RV and the LV was conducted at baseline, after adding sea anemone venom (ATX-II, 20 nmol/L), after adding apamin (100 nmol/L) in the continued presence of ATX-II and after washout. ATX-II is a specific late sodium channel (I_{NaL}) enhancer.[16] This protocol was done in 4 males and 7 females.

Statistical analysis

APD_{80} was optically measured at the level of 80% repolarization. Calcium transient duration at the level of 80% (Ca_iTD_{80}) were used as the index of total Ca_i duration. We averaged the APD in the region of interests and presented them in summary data. Continuous variables were expressed as mean ± SEM. Paired t-tests were used to compare two different treatments in the same rabbit ventricle. One-way repeated measures ANOVA with post-hoc tests were used to compare the means among three or more different variables. We used the correlation of variance generated from the optically imaged region to quantify APD heterogeneity.[17] A two-sided P value of <0.05 was considered as statistically significant.

Results

diLQTS is associated with I_{KAS} activation in female ventricles

We were unable to measure heart rate-controlled QT intervals at a fixed pacing cycle lengths (PCLs) because of the superimposition of the atrial pacing artifacts with the terminal portion of the preceding T wave. Representative examples of pECG recordings and QT interval measured during sinus rhythm are shown in Figure 1A and Figure 1B, respectively. HMR1556, E4031 and ATX-II all significantly prolonged RR interval (reduced sinus heart rate) in these female hearts. Figure 1C shows that all 3 drugs significantly increased the average RR intervals and the sinus QT intervals. T-wave end was determined by tangent method as shown in Figure 1B.[18] Apamin further prolonged sinus QT intervals, indicating the diLQT 1-3 were associated with the increased I_{KAS}. However, apamin failed to prolong QT intervals in male hearts (Online Supplement Figure 2). The other sinus rhythm parameters (P, PR, and QRS) were not changed by drug treatments. Figure 2 shows the changes (delta) of RR and QT intervals from baseline in female hearts, showing significant increments after drugs and further increase after apamin. Table 1A shows the actual QT intervals of male and female hearts measured during sinus rhythm. We have removed 2 (1 male and 1 female) hearts with diLQT1, 2 (both female) from diLQT2 and 2 (both male) from diLQT3 groups due to third degree AV block. The data from those hearts were excluded from analyses. Figure 3A shows that the APD_{80} was increased by HMR1556 (100 nmol/L) at all PCLs. However, the increases were more apparent at longer PCL (350 ms) than at shorter PCLs (300 and 250 ms). The APD_{80} was further increased by apamin (100 nmol/L) (Figure 3B and 3C). Table 1B shows HMR1556 prolonged the APD_{80} in female ventricles. These results indicated that I_{KAS} is functionally elevated during the diLQT1 at longer PCLs. Similar results were demonstrated in the diLQT2 model as shown in Figure 4. E4031 (50 nmol/L), the I_{Kr} blocker, significantly prolonged APD_{80}. While female ventricles had greater prolongation than male ventricles, the difference was statistically insignificant (Table 1B). Subsequent addition of apamin further increased the APD_{80}. The numeric results are displayed in Table 1B. Figure 4C shows that APD_{80} was significantly lengthened by E4031 at PCLs longer than 250 ms.

Figure 5A shows a representative example of optical mapping and APD traces at baseline, after infusion of ATX-II (20 nmol/L), after apamin and after washout. At PCL 350 ms, ATX-II significantly prolonged APD and subsequent addition of apamin (100 nmol/L) in the

continued presence of ATX-II in the perfusate further lengthened APD_{80} at the long, but not short, PCLs (Figure 5B and 5C).

I_{KAS} was not significantly activated in male diLQTS hearts

We applied the same protocol in male hearts but failed to observe APD prolongation after apamin administration in diLQTS (PCL 350 ms). No apamin effects were observed in the diLQT1, diLQT2, and diLQT3 models of male rabbit hearts (Figure 6). Table 1A shows the numeric values of the QT interval changes. Online Supplement Figures 3-5 show typical examples of experiments in male rabbit hearts. They showed that while all 3 drugs prolonged APD_{80} especially at longer PCLs, addition of apamin failed to further prolong APD_{80}. The numeric values are summarized in Table 1B. These results indicated that I_{KAS} is magnified in female but not in male ventricles of diLQTS. Apamin did not induce further changes of the APD heterogeneity in female diLQTS ventricles (PCL350 ms) (Online supplement Figure 6).

Apamin had little effects on intracellular calcium transient duration (Ca_iTD)

Ca_i mapping was simultaneously performed and analyzed (Figure 7). Compared with baseline, HMR1556 (100 nmol/L), E4031 (50 nmol/L) and ATX-II (20 nmol/L) markedly prolonged Ca_i transient duration. The numeric values are summarized in Table 1C. These findings indicate that Ca_iTD was significantly prolonged in diLQT1, diLQT2 and diLQT3. The E4031 prolonged CaiTD to a greater extent in female than in male ventricles, but the difference was statistically insignificant. Apamin (100 nmol/L) had a minimal further effect on Ca_iTD prolongation. The sex differences of I_{KAS} activation could not be explained by the differential prolongation of Ca_iTD in male and female ventricles.

Discussion

We found that I_{KAS} is abundantly increased in female but not in male rabbit ventricles with diLQTS. I_{KAS} activation helps preserve the repolarization reserve in female ventricles treated with I_{Ks} and I_{Kr} blockers or I_{NaL} activators. A clinical implication is that I_{KAS} blockers may be proarrhythmic in female ventricles.

Significance of I_{KAS} activation in female diLQTS

As compared with men, women have longer rate-corrected QT intervals and are more prone to QT interval prolongation and Torsade de Pointes (TdP) ventricular arrhythmias after treatment with drugs that inhibit K^+ channels.[19-21] A detailed understanding of proarrhythmic potential of ionic channel blockade is an important step towards the development of better antiarrhythmic strategy in female patients. The diLQTS is the single most common cause for withdrawal or restriction of the use of drugs already marketed.[1] Common mechanisms of diLQTS include I_{Ks} and/or I_{Kr} blockade [2, 3] as well as I_{NaL} activation,[22] although many other mechanisms also play a role.[7] In rabbit models of diLQT2, adult females had significantly lower I_{Kr} and, perhaps, inward rectifying K^+ current, which contributed to their longer QT interval and greater arrhythmia vulnerability compared with male rabbit counterpart.[23] The present consensus is that normal female hearts express fewer functional K^+ channels, resulting in longer APD.[24] When treated with

agents that inhibit I_{Kr}, adult females have a greater vulnerability to early afterdepolarizations (EAD) and TdP. More recent studies showed that rare variations in genes responsible for congenital arrhythmia syndromes are frequently found in diLQTS.[7, 8] In addition to genetic variations, disease states such as heart failure are also a prominent risk factor of diLQTS.[1]

I_{KAS} blockade and QT prolongation

Heart failure is a disease condition associated with significant SK channel upregulation. While I_{KAS} is inactive or only minimally active in normal ventricles,[9, 25] it is increased in heart failure.[12, 26, 27] Failing ventricles have decreased K^+ currents, increased I_{NaL}, reduced repolarization reserve and increased QT interval.[28] In the meantime, it activates I_{KAS} to preserve the repolarization reserve. Sex-specific I_{KAS} activation in the female ventricle helps to preserve repolarization reserve when other K^+ channels are suppressed or I_{NaL} is activated by drugs. Therefore, drugs that block I_{KAS} may be more proarrhythmic in women than in men. One of the known cardiac I_{KAS} blocker is ondansetron.[29] Consistent with the importance of I_{KAS} in female ventricles, female sex is a major risk factor for QT prolongation induced by ondansetron in patients with cardiovascular diseases.[30]

Ca_i prolongation accompanied with diLQTS as a factor for I_{KAS} activation

Cardiac repolarization alternans often precedes life-threatening ventricular arrhythmias. In alternans, Ca_i and V_m are coupled either positively (large Ca_i transient prolongs APD of the same beat) or negatively (large Ca_i transient shortens APD of the same beat).[31] V_m and Ca_i are coupled via calcium sensitive currents, such as I_{CaL}, I_{NCX}, I_{Ks} and I_{KAS}.[31, 32] The results of our study showed positive Ca_i-V_m coupling in diLQTS. The increased APD resulted in increased Ca_iTD, which in turn may contribute to the activation of calcium sensitive potassium currents, such as I_{Ks} and I_{KAS}. In diLQT1 when I_{Ks} is inhibited, the I_{KAS} may help maintain the repolarization reserve. However, Ca_iTD prolongation occurred both in male and female ventricles and the magnitudes of prolongation were not different between sexes. These findings indicate that sex-specific I_{KAS} elevation is not secondary to differential prolongation of Ca_iTD.

I_{KAS} blockade enhanced sinus bradycardias in diLQTS

Apamin is known to slow diastolic depolarization and reduce pacemaker rate in isolated sinoatrial node cells and intact tissue.[33] We found that apamin amplified the diLQT-induced heart rate slowing. The effects of apamin on APD_{80} was greater in slower heart rates than in faster heart rates. The rate-dependent increase of I_{KAS} suggests that I_{KAS} is particularly important during bradycardia to maintain repolarization reserve. I_{KAS} blockade might increase the arrhythmic risk in women with bradycardia.

Study limitations

Our findings imply that I_{KAS} is activated in female but not in male ventricles during diLQTS. A possible contributing factor is that the subtype-2 SK channel protein expression was significantly higher in female than male rabbit ventricles.[14] Furthermore, $I_{Ca,L}$ is approximately 30% higher in female than male rabbit ventricles.[24] The increased $I_{Ca,L}$ could facilitate the activation of the I_{KAS}.[34] A limitation of the present study is that we did not

directly measure the $I_{Ca,L}$ in males and females to test the latter hypothesis. Apamin does not block any known major cardiac potassium currents.[35] However, because of molecular diversity of potassium channel genes in the myocardium,[36] the specificity of apamin cannot be determined until all cardiac potassium channel genes are completely characterized.

Conclusions

We conclude that I_{KAS} is abundantly increased in female but not in male ventricles with diLQTS. Increased I_{KAS} helps preserve the repolarization reserve in female ventricles treated with I_{Ks} and I_{Kr} blockers or I_{NaL} activators.

Supplementary Material

Refer to Web version on PubMed Central for supplementary material.

Acknowledgements

This work was supported by NIH R01 (HL139829, R42DA043391, TR002208-01), the American Heart Association grant (18TPA34170284), a Charles Fisch Research Award endowed by Dr Suzanne B. Knoebel, a Medtronic-Zipes Endowment, and the Indiana University Health-Indiana University School of Medicine Strategic Research Initiative. We thank Nicole Courtney, Chris Corr, and David Adams for their assistances.

References

1. Roden DM. Drug-induced prolongation of the QT interval. N Engl J Med 2004;350:1013–1022. [PubMed: 14999113]
2. Mitcheson JS, Chen J, Lin M, Culberson C, Sanguinetti MC. A structural basis for drug-induced long QT syndrome. Proc Natl Acad Sci U S A 2000;97:12329–12333. [PubMed: 11005845]
3. Pollard CE, Abi Gerges N, Bridgland-Taylor MH, Easter A, Hammond TG, Valentin JP. An introduction to QT interval prolongation and non-clinical approaches to assessing and reducing risk. Br J Pharmacol 2010;159:12–21. [PubMed: 20141516]
4. Priori SG, Wilde AA, Horie M, et al. HRS/EHRA/APHRS expert consensus statement on the diagnosis and management of patients with inherited primary arrhythmia syndromes. Heart Rhythm 2013;10:1932–1963. [PubMed: 24011539]
5. Lehtonen A, Fodstad H, Laitinen-Forsblom P, Toivonen L, Kontula K, Swan H. Further evidence of inherited long QT syndrome gene mutations in antiarrhythmic drug-associated torsades de pointes. Heart Rhythm 2007;4:603–607. [PubMed: 17467628]
6. Kaab S, Crawford DC, Sinner MF, et al. A large candidate gene survey identifies the KCNE1 D85N polymorphism as a possible modulator of drug-induced torsades de pointes. Circ Cardiovasc Genet 2012;5:91–99. [PubMed: 22100668]
7. Ramirez AH, Shaffer CM, Delaney JT, et al. Novel rare variants in congenital cardiac arrhythmia genes are frequent in drug-induced torsades de pointes. Pharmacogenomics J 2013;13:325–329. [PubMed: 22584458]
8. Weeke P, Mosley JD, Hanna D, et al. Exome sequencing implicates an increased burden of rare potassium channel variants in the risk of drug-induced long QT interval syndrome. J Am Coll Cardiol 2014;63:1430–1437. [PubMed: 24561134]
9. Nagy N, Szuts V, Horvath Z, et al. Does small-conductance calcium-activated potassium channel contribute to cardiac repolarization? J Mol Cell Cardiol 2009;47:656–663. [PubMed: 19632238]
10. Zhang XD, Lieu DK, Chiamvimonvat N. Small-conductance Ca2+ -activated K+ channels and cardiac arrhythmias. Heart Rhythm 2015;12:1845–1851. [PubMed: 25956967]
11. Chang PC, Chen PS. SK channels and ventricular arrhythmias in heart failure. Trends Cardiovasc Med 2015;25:508–514. [PubMed: 25743622]

12. Chua SK, Chang PC, Maruyama M, et al. Small-conductance calcium-activated potassium channel and recurrent ventricular fibrillation in failing rabbit ventricles. Circ Res 2011;108:971–979. [PubMed: 21350217]
13. Lee YS, Chang PC, Hsueh CH, et al. Apamin-sensitive calcium-activated potassium currents in rabbit ventricles with chronic myocardial infarction. J Cardiovasc Electrophysiol 2013;24:1144–1153. [PubMed: 23718850]
14. Chen M, Yin D, Guo S, et al. Sex-specific activation of SK current by isoproterenol facilitates action potential triangulation and arrhythmogenesis in rabbit ventricles. J Physiol 2018;596:4299–4322. [PubMed: 29917243]
15. Koller ML, Riccio ML, Gilmour RF Jr. Dynamic restitution of action potential duration during electrical alternans and ventricular fibrillation. Am J Physiol 1998;275:H1635–1642. [PubMed: 9815071]
16. el-Sherif N, Fozzard HA, Hanck DA. Dose-dependent modulation of the cardiac sodium channel by sea anemone toxin ATXII. Circ Res 1992;70:285–301. [PubMed: 1346508]
17. Yin D, Yang N, Tian Z, et al. Ondansetron effects on apamin-sensitive small conductance calcium-activated potassium currents in pacing induced failing rabbit hearts. Heart Rhythm 2019.
18. Postema PG, Wilde AA. The measurement of the QT interval. Curr Cardiol Rev 2014;10:287–294. [PubMed: 24827793]
19. Makkar RR, Fromm BS, Steinman RT, Meissner MD, Lehmann MH. Female gender as a risk factor for torsades de pointes associated with cardiovascular drugs. JAMA 1993;270:2590–2597. [PubMed: 8230644]
20. Burke JH, Ehlert FA, Kruse JT, Parker MA, Goldberger JJ, Kadish AH. Gender-specific differences in the QT interval and the effect of autonomic tone and menstrual cycle in healthy adults. Am J Cardiol 1997;79:178–181. [PubMed: 9193019]
21. Drici MD, Knollmann BC, Wang WX, Woosley RL. Cardiac actions of erythromycin: influence of female sex. JAMA 1998;280:1774–1776. [PubMed: 9842954]
22. Yang T, Chun YW, Stroud DM, et al. Screening for acute IKr block is insufficient to detect torsades de pointes liability: role of late sodium current. Circulation 2014;130:224–234. [PubMed: 24895457]
23. Liu XK, Katchman A, Drici MD, et al. Gender difference in the cycle length-dependent QT and potassium currents in rabbits. J Pharmacol Exp Ther 1998;285:672–679. [PubMed: 9580612]
24. Sims C, Reisenweber S, Viswanathan PC, Choi BR, Walker WH, Salama G. Sex, age, and regional differences in L-type calcium current are important determinants of arrhythmia phenotype in rabbit hearts with drug-induced long QT type 2. Circ Res 2008;102:e86–100. [PubMed: 18436794]
25. Tuteja D, Xu D, Timofeyev V, et al. Differential expression of small-conductance Ca2+-activated K + channels SK1, SK2, and SK3 in mouse atrial and ventricular myocytes. Am J Physiol Heart Circ Physiol 2005;289:H2714–2723. [PubMed: 16055520]
26. Bonilla IM, Long VP 3rd, Vargas-Pinto P, et al. Calcium-activated potassium current modulates ventricular repolarization in chronic heart failure. PLoS One 2014;9:e108824. [PubMed: 25271970]
27. Yu CC, Corr C, Shen C, et al. Small conductance calcium-activated potassium current is important in transmural repolarization of failing human ventricles. Circ Arrhythm Electrophysiol 2015;8:667–676. [PubMed: 25908692]
28. Nattel S The heart on a chip: the role of realistic mathematical models of cardiac electrical activity in understanding and treating cardiac arrhythmias. Heart Rhythm 2007;4:779–780. [PubMed: 17556202]
29. Ko JS, Guo S, Hassel J, et al. Ondansetron blocks wild-type and p.F503L variant small-conductance Ca(2+)-activated K(+) channels. Am J Physiol Heart Circ Physiol 2018;315:H375–H388. [PubMed: 29677462]
30. Hafermann MJ, Namdar R, Seibold GE, Page RL 2nd. Effect of intravenous ondansetron on QT interval prolongation in patients with cardiovascular disease and additional risk factors for torsades: a prospective, observational study. Drug Healthc Patient Saf 2011;3:53–58. [PubMed: 22046106]

31. Weiss JN, Karma A, Shiferaw Y, Chen PS, Garfinkel A, Qu Z. From pulsus to pulseless: the saga of cardiac alternans. Circ Res 2006;98:1244–1253. [PubMed: 16728670]
32. Kennedy M, Bers DM, Chiamvimonvat N, Sato D. Dynamical effects of calcium-sensitive potassium currents on voltage and calcium alternans. J Physiol 2017;595:2285–2297. [PubMed: 27902841]
33. Torrente AG, Zhang R, Wang H, et al. Contribution of small conductance K+ channels to sinoatrial node pacemaker activity: insights from atrial-specific Na+ /Ca2+ exchange knockout mice. J Physiol 2017;595:3847–3865. [PubMed: 28346695]
34. Zhang XD, Coulibaly ZA, Chen WC, et al. Coupling of SK channels, L-type Ca(2+) channels, and ryanodine receptors in cardiomyocytes. Sci Rep 2018;8:4670. [PubMed: 29549309]
35. Yu CC, Ai T, Weiss JN, Chen PS. Apamin does not inhibit human cardiac Na+ current, L-type Ca2+ current or other major K+ currents. PLoS One 2014;9:e96691. [PubMed: 24798465]
36. Nerbonne JM. Molecular basis of functional voltage-gated K+ channel diversity in the mammalian myocardium. J Physiol 2000;525 Pt 2:285–298. [PubMed: 10835033]

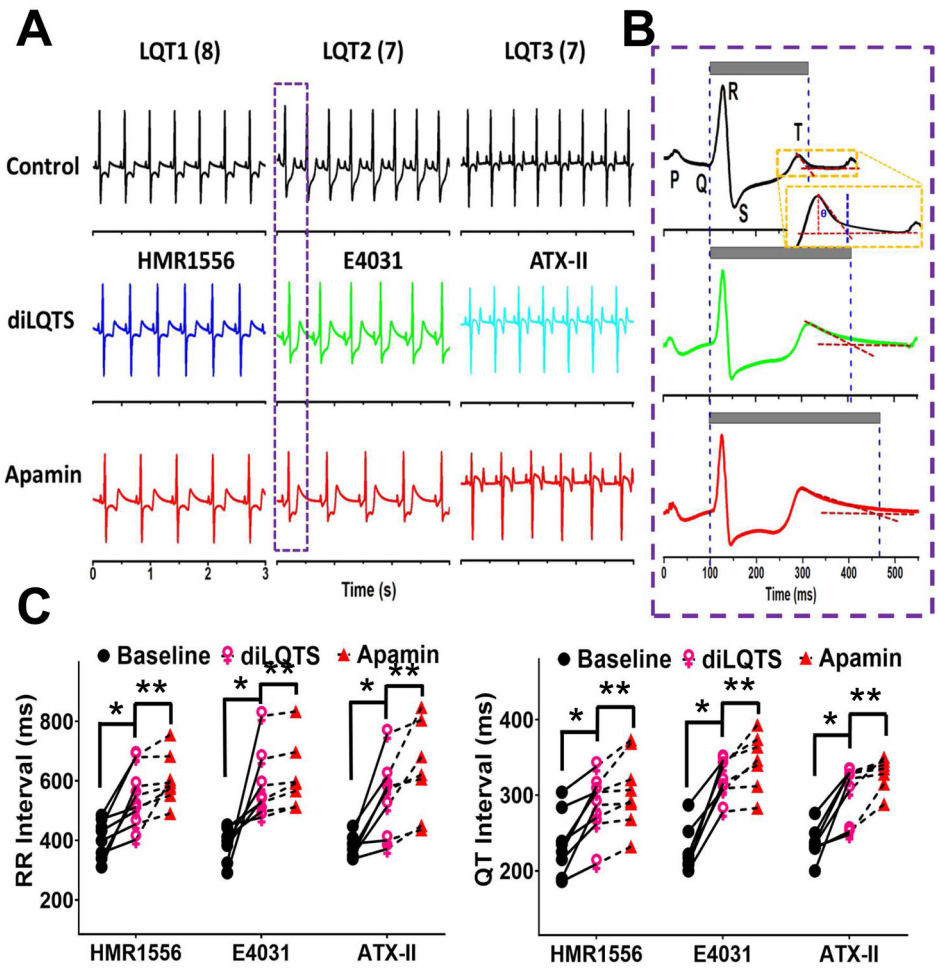

Figure 1.

Sinus bradycardia of diLQT1, diLQT2 and diLQT3 in *ex vivo* female rabbit hearts. **A,** representative pseudo ECG traces of diLQT1 (HMR1556, 100 nmol/L), diLQT2 (E4031, 50 nmol/L), and diLQT 3 (ATX-II, 20 nmol/L). Apamin (100 nmol/L) was then given during continued drug infusion. **B,** magnified figures showing the typical ECG traces from the box in (A), schematic illustration of the tangent method to define the T-wave end. The gray bars indicate the QT interval. **C,** Linkage graphs show the alterations of the RR and QT intervals in different types of diLQTS. There are significant ($p<0.05$) differences between baseline and diLQTS (*) as well as between diLQTS and post-apamin (**).

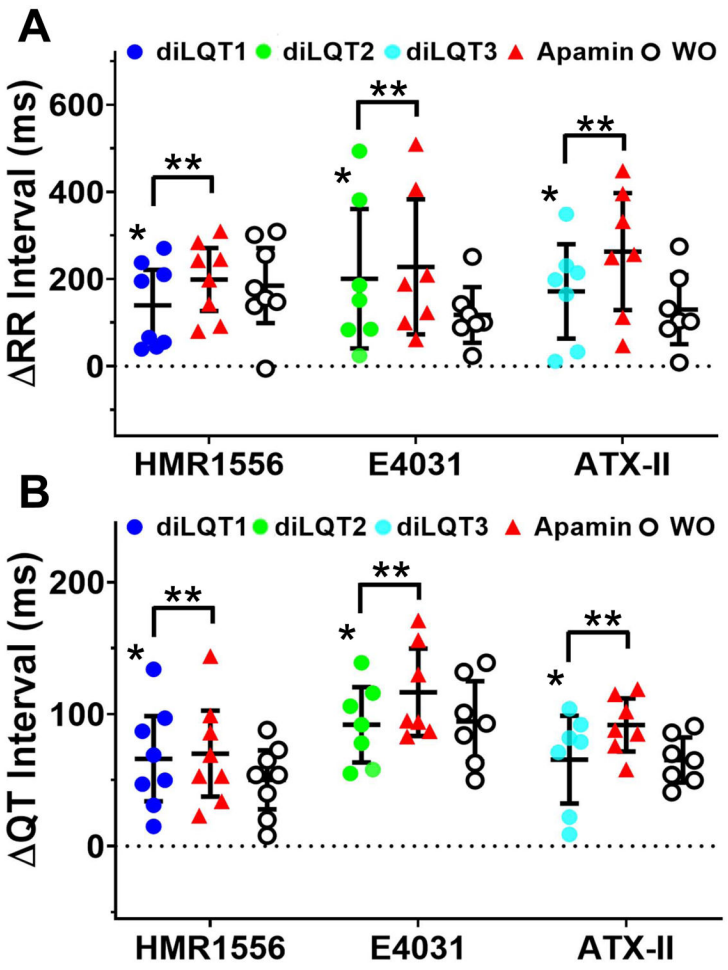

Figure 2.

Effects of drugs and apamin on RR and QT intervals in female hearts. **A,** differences (delta) in RR intervals between treatments and baseline. The delta between RR interval and baseline was statistically significant both after drug and after apamin. **B,** the delta QT interval at different stages of the experiment. The delta QT interval was increased by the drugs and by apamin. The RR and QT intervals were only partially reduced after attempted washout (WO). Asterisks (*diLQTS compared with baseline; **diLQTS compared with post-apamin) represent significant differences ($p<0.05$, each n=7-8).

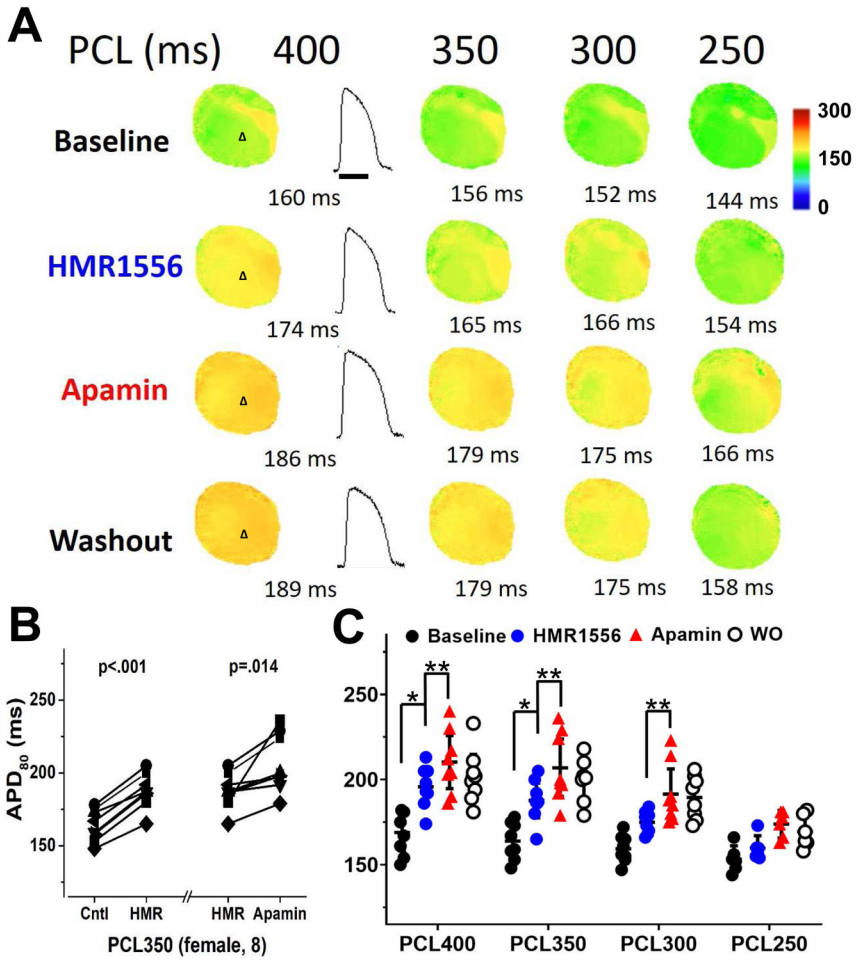

Figure 3.

Changes in APD_{80} in female ventricles treated with HMR1556 followed by apamin and washout in a female heart. **A,** the color maps show epicardial APD distribution at different pacing cycle lengths (PCLs). HMR1556 (100 nmol/L) increased APD_{80}. Apamin (100 nmol/L) further increased the APD_{80}, and after washout (Protocol I, diLQT1). **B,** HMR1556 prolonged APD_{80}. Addition of apamin further increased the APD_{80}. APD_{80} is persistently prolonged after washout (WO). **C,** summary of these studies at different PCLs. The magnitude of APD prolongation by HMR1556 was more prominent at long PCLs than at short PCLs. The apamin further prolonged APD_{80} at multiple PCLs. Data presented as mean ± SEM. Asterisks (*diLQTS compared with baseline; **diLQTS compared with post-apamin) represent significant differences ($p<0.05$, n=8).

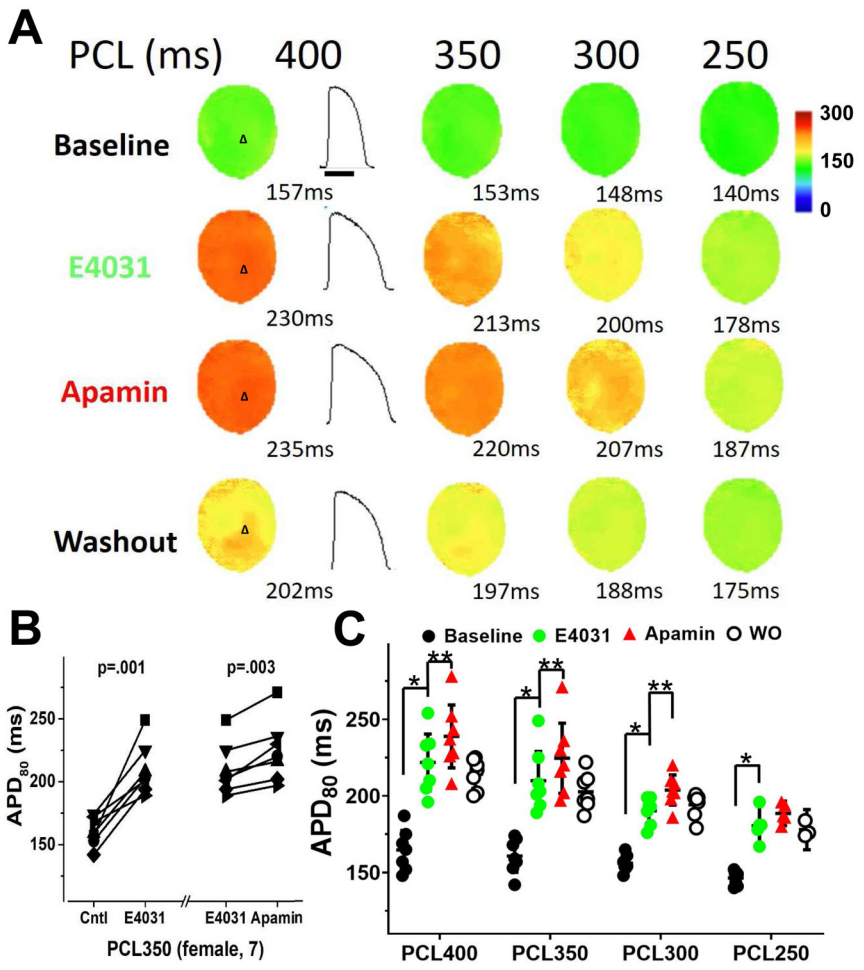

Figure 4.

Changes in APD_{80} in female ventricles treated with E4031 followed by apamin and washout. **A,** representative membrane potential traces and APD_{80} maps at baseline and in the presence of E4031 (50 nmol/L), after apamin (100 nmol/L), and after washout (Protocol II, diLQT2). **B,** at 350 ms PCL, E4031 (50 nmol/L) significantly prolonged APD_{80} and apamin further increased the APD_{80}. APD_{80} is persistently prolonged after washout (WO). **C,** summary of apamin effects on APD_{80} at different PCLs. Significant effects of apamin were observed at all but 250 ms PCLs. Asterisks (*diLQTS compared with baseline; **diLQTS compared with post-apamin) represent significant differences ($p<0.05$, n=7).

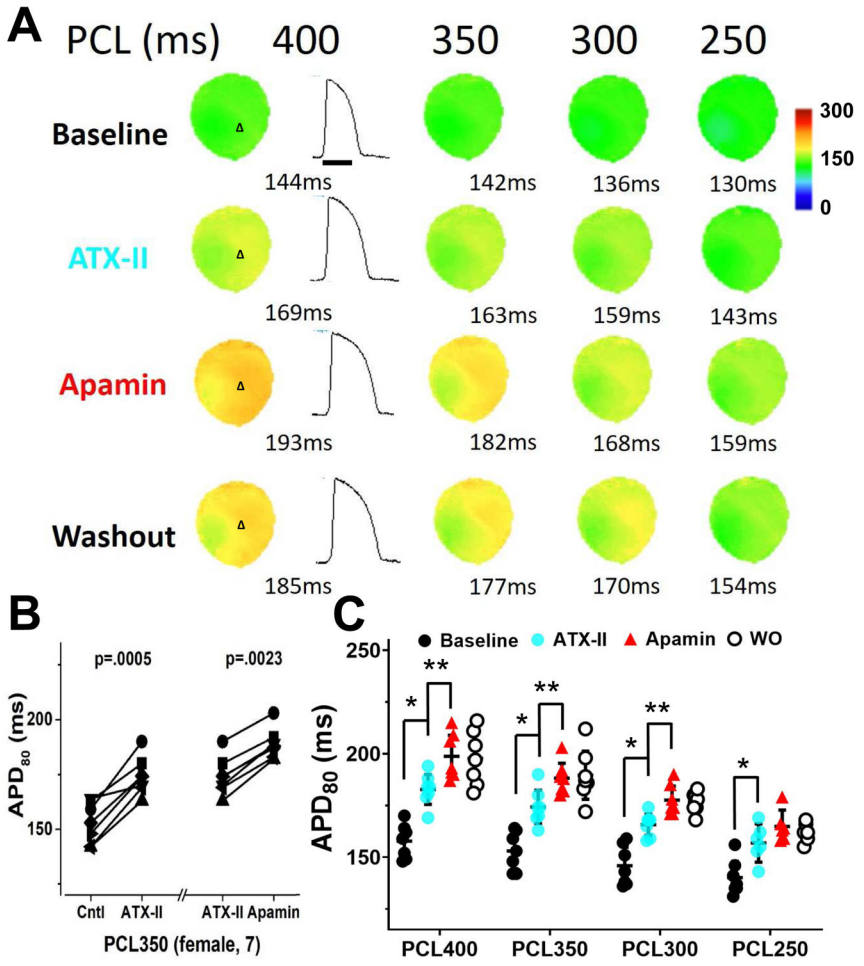

Figure 5.

Changes in APD_{80} in female ventricles treated with ATX-II followed by apamin and washout. **A,** representative membrane potential traces and APD_{80} maps at baseline and in the presence of ATX-II (20 nmol/L), after apamin (100 nmol/L), and after washout (Protocol III, diLQT3). **B,** at 350 ms PCL, ATX-II significantly prolonged APD_{80} and apamin then further increased the APD_{80}. APD_{80} is persistently prolonged after washout (WO). **C,** summary of apamin effects on APD_{80} at different PCLs in normal rabbit ventricles. The apamin effects were observed at multiple PCLs but not in 250 ms PCL. Asterisks (*diLQTS compared with baseline; **diLQTS compared with post-apamin) represent significant differences ($p<0.05$, n=7).

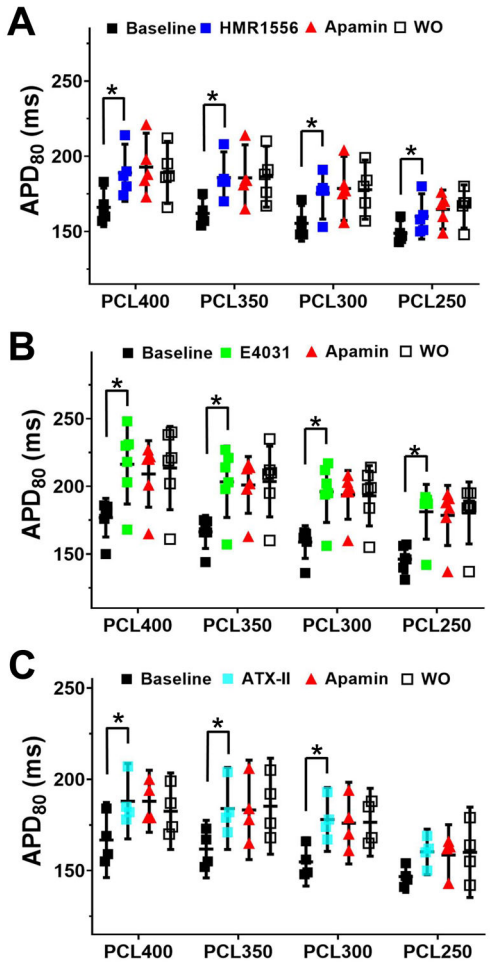

Figure 6.

Apamin did not prolong APD_{80} in male ventricles with diLQT1 (**A**), diLQT2 (**B**) and diLQT3 (**C**). There were significant APD_{80} prolongations after drug administration, especially at longer PCLs. However, no further prolongation was observed after apamin, indicating absence of I_{KAS} activation in male diLQTS model. Asterisks indicate significant differences ($p<0.05$, each n=4-6).

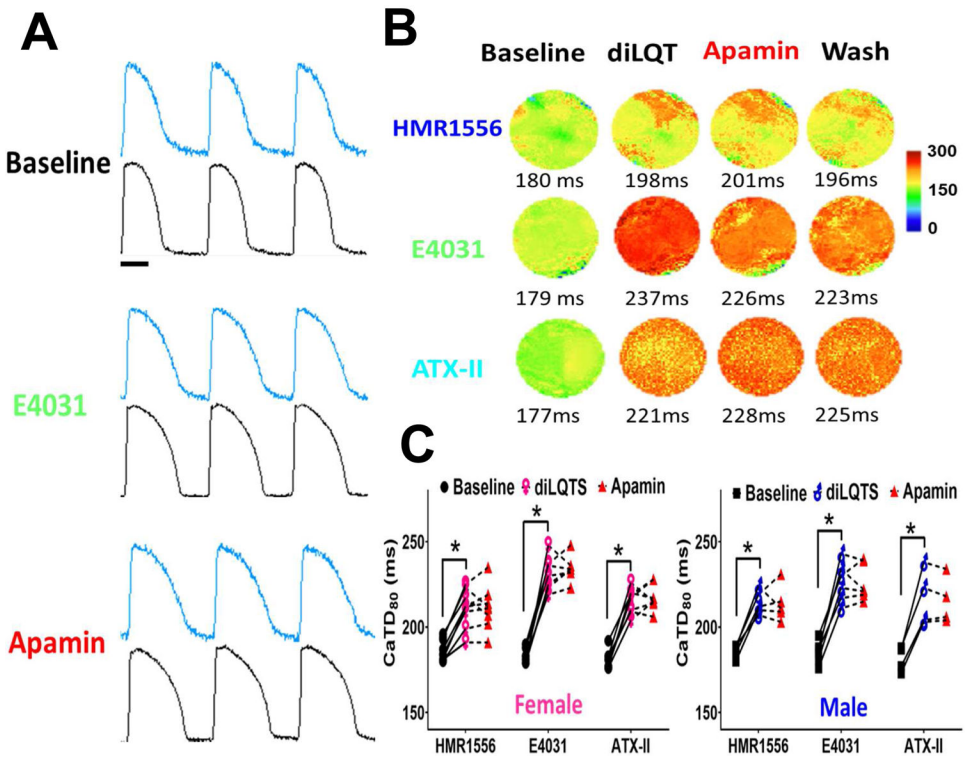

Figure 7.

Effects of I_{KAS} blockade on Ca_iTD in diLQTS models. **A,** representative Ca_i (blue) and V_m (black) traces at baseline, during E4031, and after apamin (Protocol-II) at 350 ms PCL in a female heart. Compared with baseline, E4031 (50 nmol/L) markedly prolonged Ca_iTD_{80}. Apamin (100 nmol/L) only slightly prolonged Ca_iTD, but the prolongation was statistically insignificant. **B,** representative Ca_iTD distribution maps of diLQT1 (top), diLQT2 (middle) and diLQT3 (bottom) with female hearts treated with HMR1556 (100 nmol/L), E4031 (50 nmol/L) or ATX-II (20 nmol/L), respectively, at 350 ms PCL. Addition of apamin (100 nmol/L) did not further prolong the Ca_iTD. **C,** linkage graphs show the alterations of the Ca_iTD_{80} in different types of diLQTS, neither male nor female ventricles showed Ca_iTD_{80} prolongation after adding apamin at 350 ms PCL. Asterisks indicate significant differences ($p<0.05$, each n=4-8).

Table 1.

Effects of apamin on repolarization and calcium transients

A. ECG QT intervals during sinus rhythm

Type	Sex	Sinus QT	QT (diLQTS)	QT (apamin)	n
I_{Ks} (HMR1556)	Male	229.8 ± 11.6	295.4 ± 17.1 *	303.4 ± 18.9	5
	Female	220.8 ± 7.8	284.5 ± 14.9 *	304.6 ± 18.1 **	8
I_{Kr} (E4031)	Male	235.7 ± 8.6	319.2 ± 12.3 *	325.8 ± 11.7	6
	Female	228.0 ± 11.7	320.0 ± 9.4 *	344.6 ± 14.2 **	7
$I_{Na,L}$ (ATX-II)	Male	221.3 ± 11.3	287.3 ± 8.4 *	293.5 ± 6.6	4
	Female	234.4 ± 6.3	302.1 ± 13.8 *	328.7 ± 8.1 **	7

*p<0.05 compared with baseline; **p<0.05 compared with diLQTS; time scale: ms.

B. Optical mapping APD during atrial pacing with cycle length of 350 ms

Type	Sex	Baseline APD_{80}	ΔAPD_{80} (diLQTS)	ΔAPD_{80} (apamin)	n
I_{Ks} (HMR1556)	Male	162.0 ± 3.6	23.8 ± 3.0 *	−0.2 ± 1.8	5
	Female	163.9 ± 3.9	23.9 ± 1.9 *	19.1 ± 5.9 **	8
I_{Kr} (E4031)	Male	166.3 ± 4.8	37.0 ± 6.0 *	−2.3 ± 2.8	6
	Female	160.7 ± 4.3	49.1 ± 8.0 *	14.7 ± 2.9 **	7
$I_{Na,L}$ (ATX-II)	Male	161.8 ± 5.5	22.3 ± 3.9 *	−0.8 ± 1.5	4
	Female	158.0 ± 3.5	21.3 ± 2.9 *	13.9 ± 1.6 **	7

*p<0.05 compared with baseline; **<0.05 compared with males; time scale: ms.

C. Optical mapping Ca_iTD during atrial pacing with cycle length of 350 ms

Type	Sex	Baseline Ca_iTD_{80}	ΔCa_iTD_{80} (diLQTS)	ΔCa_iTD_{80} (apamin)	n
I_{Ks} (HMR1556)	Male	185.0 ± 1.6	29.4 ± 3.3 *	−0.6 ± 4.1	5
	Female	184.5 ± 2.6	26.5 ± 1.8 *	1.6 ± 3.4	8
I_{Kr} (E4031)	Male	185.3 ± 2.6	41.0 ± 4.1 *	−0.2 ± 2.9	6
	Female	182.7 ± 1.7	48.4 ± 4.1 *	3.3 ± 3.1	7
$I_{Na,L}$ (ATX-II)	Male	181.5 ± 3.6	35.5 ± 5.5 *	−1.5 ± 1.8	4
	Female	181.3 ± 2.1	33.7 ± 3.0 *	2.6 ± 3.2	7

*p<0.05 compared with baseline; time scale: ms.